

# Synchronous Rectification Control in CLLC Converters Based on Hall-Effect Current Sensors



Vsevolod Elantsev

Power converters based on soft-switching topologies are rising in popularity. Resonant converters, such as LLC and CLLC, have soft-switching operation and achieve a high switching frequency and offer high power density. Conversely, a high switching frequency can add additional complexity in the system. The CLLC converter is a bidirectional topology and is widely used in [solar inverters](#) and [battery energy storage systems](#). To achieve higher efficiency and lower power dissipation, implement a synchronous rectification (SR) on the secondary side of a converter. Measure the current to implement the SR. Due to the high-frequency operation of the converters, traditional approaches such as shunt or current transformers, are no longer the best option due to the high propagation delays present between the measured and real current. To solve for the high propagation delays, alternatives, such as Rogowsky coils are used, however Rogowsky coils still require an external circuit. Texas Instruments offers low propagation delay, high bandwidth, and low distortion Hall effect current sensors that are an excellent fit into synchronous rectification control. This application brief proposes performance assessment of the current sensing propagation delay.

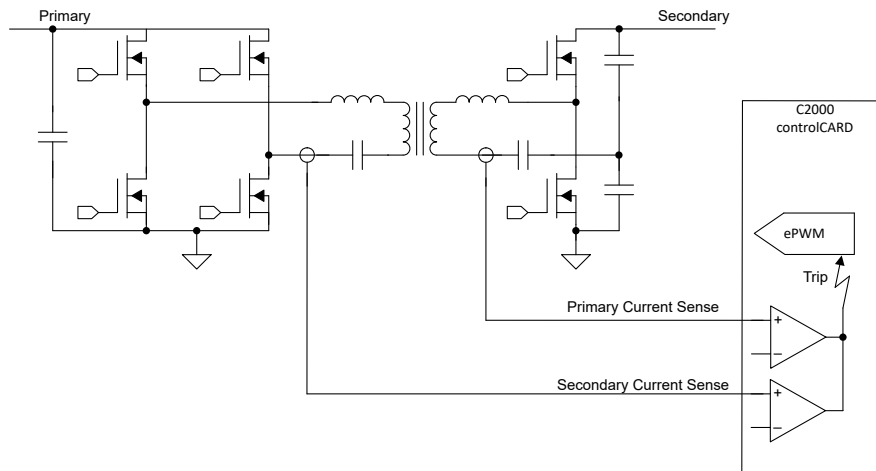
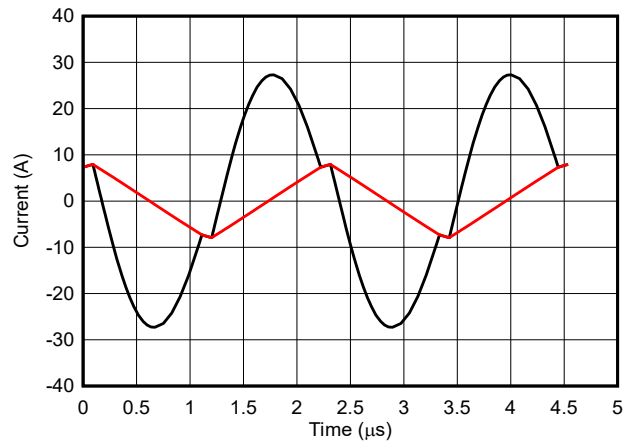
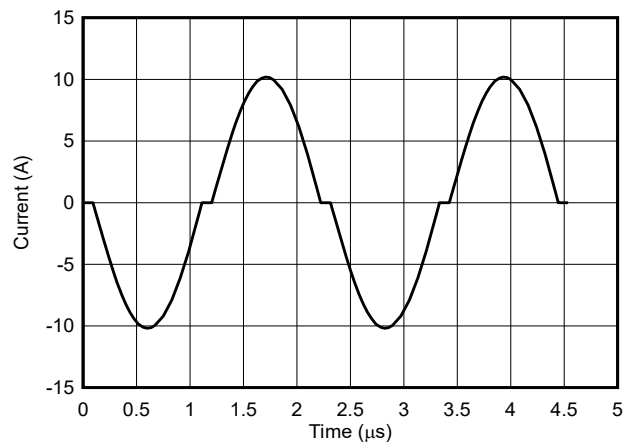


Figure 1. Control Scheme for the CLLC Converter

Some LLC converters are designed with diodes on the secondary side, a simple and inexpensive fix. The result of SR on the secondary side is complex and expensive but is more efficient and compact due to a smaller heat sink. Conversely, the converter with SR can be used to achieve bidirectional power flow. The converter with resonant tanks on both sides of the transformer is the CLLC converter. The resonant CLLC topology can be used for isolated LV-to-HV and HV-to-LV conversion in bidirectional and hybrid solar inverters.



**Figure 2. Primary Side and Magnetizing Current**



**Figure 3. Secondary Side Current**

In SR, one side of transformer operates as an excitation circuit while the other side operates as synchronous rectifier. Control the synchronous rectifier to achieve best efficiency. When operating below the resonant frequency, the primary current meets the magnetizing current and the primary-to-secondary power transfer period is shorter than the switching period. As shown in [Figure 3](#), there are periods when secondary side current is equal to zero. It is important to turn-off the SR switches when the secondary side current reaches zero, to prevent backward current flow.

The system controller needs to detect secondary side current and generate the SR control signals that are aligned with the secondary side current. The main challenge in SR control is that the synchronous rectification needs to stop as close to zero current as possible, without crossing zero. Any delays in current measurement, signal isolation and gate driver circuits complicate the control. The typical control structure of the SR control is illustrated in [Figure 1](#). The primary and secondary side PWM signals are synchronized, but the secondary side PWM signals are turned off in case if the absolute value of  $I_s$  is going lower than a certain threshold (typical value is 5% of the maximum current). [Figure 4](#) is the modulation timing diagram. With the [C2000 real-time microcontrollers \(MCU\) family](#) the ePWM, CMPSS, and PWMXBAR modules can be configured so that the modulation scheme in the hardware does not have CPU involvement. As shown in [Figure 4](#), the SR PWM module connects to the CMP signal and trips when the current goes below a threshold.

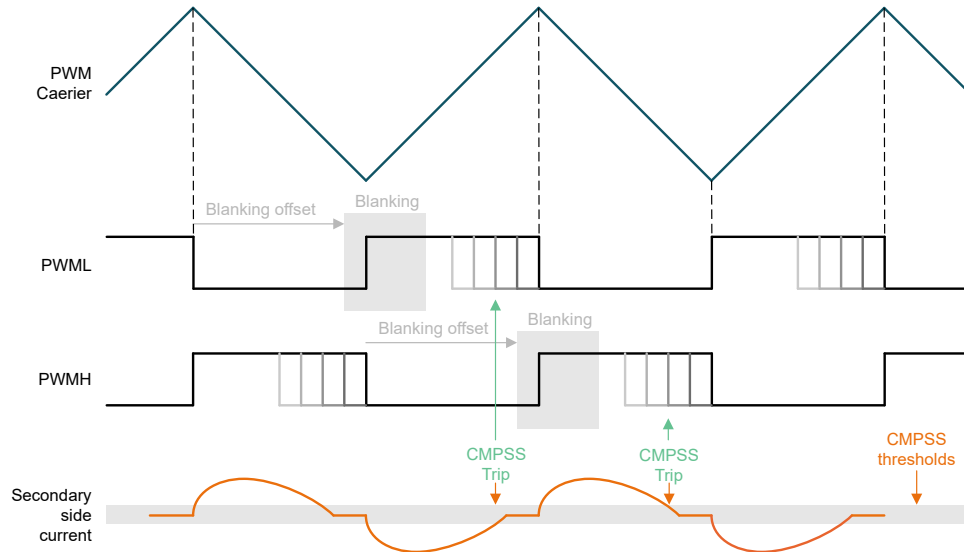


**Figure 4. Timing Diagram for CLLC Modulation**

Operating high-frequency CLLC converters above 300kHz can be challenging due to current sensing. Current sensing solutions require enough bandwidth and low latency. Traditionally, a Rogowski coil is used in SR applications. Rogowski coils require additional circuitry to convert the output current to output voltage for a comparator. [Figure 5](#) shows the solution.

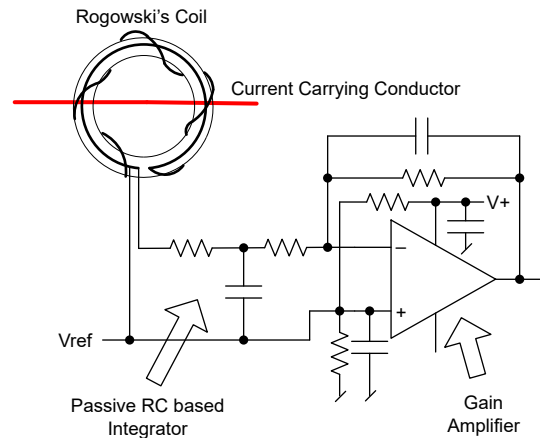


**Figure 5. Example of the Rogowski Coil Circuit**

Rogowski coil is typically custom-made and is not commercially available.

The alternative Rogowski coil is to use fast a Hall effect current sensor, such as the [TMCS1133](#). The function block diagram is shown on [Figure 6](#). TMCS1133 has a 1-MHz bandwidth and a low propagation delay of

50ns. The TMCS1133 has reinforced isolation, high immunity to external magnetic fields, and offset cancellation functionality and is good choice for synchronous rectification control.

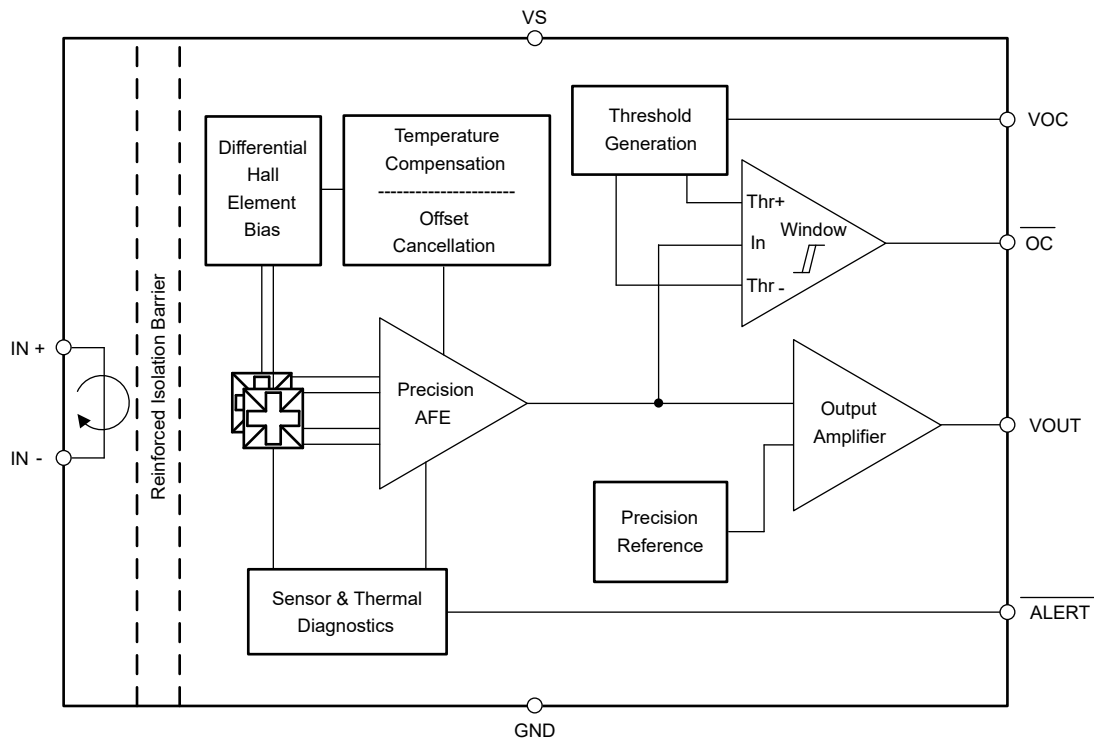


**Figure 6. TMCS1133 Hall Effect Current Sensor Diagram**

Comparing the two hall sensors shows the importance of the proper timing in the high frequency CLLC converters. The simulations have two current sensors with propagation delays of 50ns and 250ns. The converter switching frequency is 450kHz.

The waveforms for voltages and currents in power switches are shown in [Figure 7](#) and [Figure 8](#).

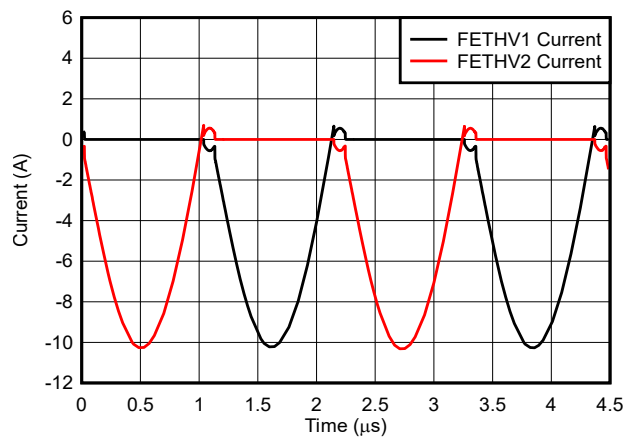


**Figure 7. Current in SR Switches with Different Propagation Delays, 50ns  $T_{PD}$**

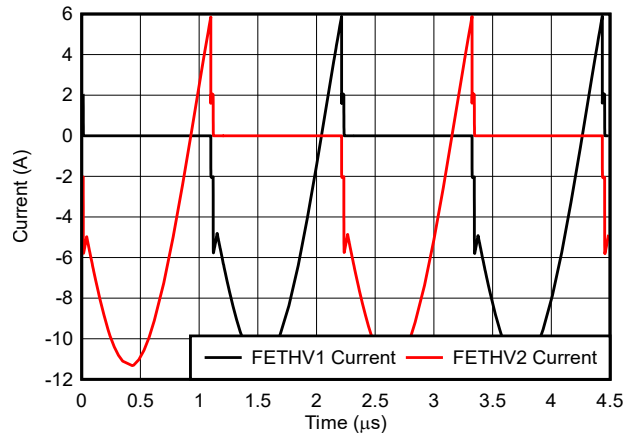


**Figure 8. Current in SR Switches with Different Propagation Delays, 250ns  $T_{PD}$**

In the best case, the secondary SR switches only has negative current in each period and switches are turned-off when secondary current reaches zero. In reality, the current in secondary side switches can go above zero and starts to push some current back to primary side. The positive current in switches causes excess reactive current and additional losses associated with the current.

In the simulations, the secondary side current with a higher  $T_{PD}$  has a larger positive amplitude. The positive current causes two main issues. First, the reactive power needs to be compensated to deliver the required output current. The active power transfer period needs to deliver more energy to the secondary side because part of the energy is transferred back to primary. The RMS current on secondary side can be significantly increased. For example, the secondary current for low 50ns  $T_{PD}$  is 4.78A<sub>RMS</sub> while the current for high for the 250ns  $T_{PD}$  is 5.45A<sub>RMS</sub>, the difference in RMS current increases conduction losses by 30 %. The RMS current increases with a further increase of  $T_{PD}$ .

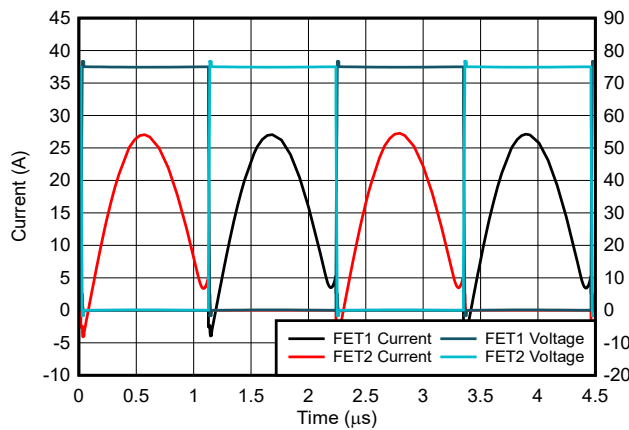


**Figure 9. Currents and Voltages in Primary Side Switches with Different Propagation Delays, 50ns  $T_{PD}$**

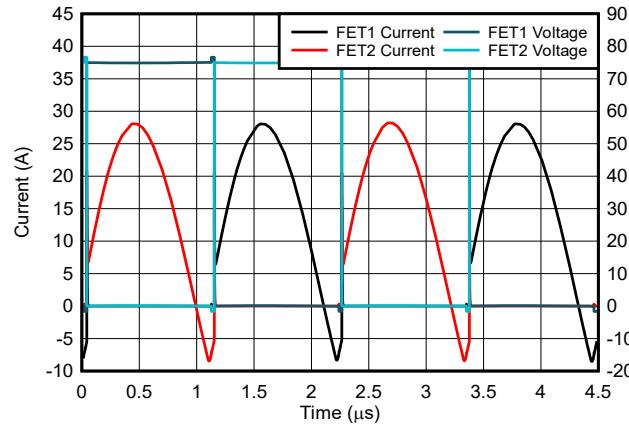


**Figure 10. Currents and Voltages in Primary Side Switches with Different Propagation Delays, 250ns  $T_{PD}$**

The second issue with the reactive current is the loss of zero voltage switching (ZVS) on primary side switches. The primary side ZVS is achieved by the magnetizing current of the transformer as shown by the red curve in [Figure 2](#). To discharge the capacitance of switches, the magnetizing current has a significant positive value in the end of the switching cycle. The effective current visible by primary side switches is reduced by the secondary side current. The primary side turn-off current can be calculated from [Equation 1](#).

$$I_{OFF, PRI} = I_M - N \times I_{SEC} \quad (1)$$

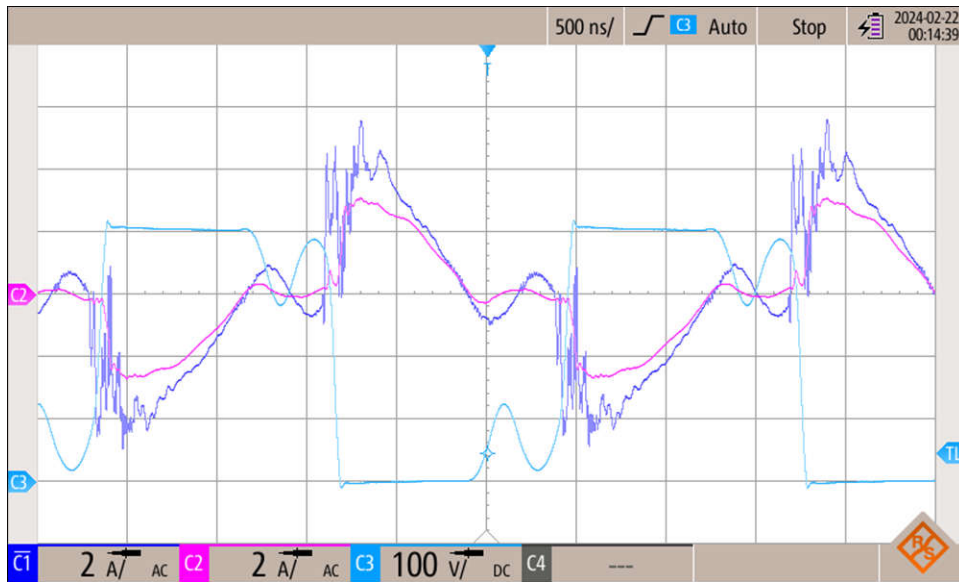
where

- $I_{OFF, PRI}$  is the turn-off current on primary side switches
- $I_M$  the magnetizing current
- $N$  is the turns ratio
- $I_{SEC}$  is the current for switches on secondary side

In case of significant backward power flow, the primary side switches can have less turn-off current than expected. In some cases, the primary side turn-off current becomes negative, causing a full hard-switch of the primary switches. As illustrated in [Figure 9](#) and [Figure 10](#), the primary side switches are in soft-switching mode with 50ns  $T_{PD}$ , and in full hard-switching with 250ns  $T_{PD}$ . Additional 4W losses are caused by hard-switching.

When 1200W is converted with 250ns  $T_{PD}$  the total losses are about 7W higher than in 50ns  $T_{PD}$  case. The efficiency of power conversion drops by 0.6% from 98.2% to 97.6%. The efficiency decrease causes a 33% increase of dissipated power.

Based on the considered simulations, the low-propagation delay Hall effect current sensors TMCS1133 are used in the [TIDA-010933](#) reference design. TMCS1133 has a low propagation delay of 50ns and is designed for use with the CLLLC converter control. The propagation delay is small enough to have almost no reactive power in the CLLLC stage. The waveforms of the SR control are shown in [Figure 11](#).



1. C1 is the TMCS1133 measurement
2. C2 is the current measurement with current probe
3. C3 is the secondary side voltage

**Figure 11. Waveforms of the Secondary Side Voltage, Current, and TMCS1133 Output on the TIDA-010933 Board**

In the waveforms, the TMCS1133 has noise and oscillations caused by a switching event, the sensors output recovers within 250ns. The noise in the beginning of the cycle can be ignored by blanking period and does not affect the final performance of the converter. The noise and delay around zero crossing is more significant for the converter's performance. After the 300ns blanking period, the best outcome is a minimal difference between the measured secondary side current and TMCS1133 output.

For high frequency SR circuits, the propagation delay of the current sensor is very important. Based on simulations, the propagation delay of  $\geq 250\text{ns}$  causes significant impact to efficiency of the 450 kHz converter. The simulations and practical experiment show that TMCS1133 is an excellent choice for high-frequency, synchronous rectifier applications because of the ultra-low propagation delay, reducing overall conversion losses and increasing power density in power conversion systems.

### Trademarks

All trademarks are the property of their respective owners.

## IMPORTANT NOTICE AND DISCLAIMER

TI PROVIDES TECHNICAL AND RELIABILITY DATA (INCLUDING DATA SHEETS), DESIGN RESOURCES (INCLUDING REFERENCE DESIGNS), APPLICATION OR OTHER DESIGN ADVICE, WEB TOOLS, SAFETY INFORMATION, AND OTHER RESOURCES "AS IS" AND WITH ALL FAULTS, AND DISCLAIMS ALL WARRANTIES, EXPRESS AND IMPLIED, INCLUDING WITHOUT LIMITATION ANY IMPLIED WARRANTIES OF MERCHANTABILITY, FITNESS FOR A PARTICULAR PURPOSE OR NON-INFRINGEMENT OF THIRD PARTY INTELLECTUAL PROPERTY RIGHTS.

These resources are intended for skilled developers designing with TI products. You are solely responsible for (1) selecting the appropriate TI products for your application, (2) designing, validating and testing your application, and (3) ensuring your application meets applicable standards, and any other safety, security, regulatory or other requirements.

These resources are subject to change without notice. TI grants you permission to use these resources only for development of an application that uses the TI products described in the resource. Other reproduction and display of these resources is prohibited. No license is granted to any other TI intellectual property right or to any third party intellectual property right. TI disclaims responsibility for, and you will fully indemnify TI and its representatives against, any claims, damages, costs, losses, and liabilities arising out of your use of these resources.

TI's products are provided subject to [TI's Terms of Sale](#) or other applicable terms available either on [ti.com](https://www.ti.com) or provided in conjunction with such TI products. TI's provision of these resources does not expand or otherwise alter TI's applicable warranties or warranty disclaimers for TI products.

TI objects to and rejects any additional or different terms you may have proposed.

Mailing Address: Texas Instruments, Post Office Box 655303, Dallas, Texas 75265  
Copyright © 2024, Texas Instruments Incorporated